IJST EXPLORE International Journal of Science and Technology
CENTRE OF PROFESSIONAL RESEARCH PUBLICATIONS
ISSN 2049-7318

International Journal of Science and Technology Volume 2 No. 8, August, 2013

# Effect of Strain Rates on Mild Steel under Tensile Loading

**Ogundare O.D., Momoh I.M., Akinribide O.J., Daniyan, A.A., [1,2] Adetunji, A.R., Olusunle, S.O.O.**
Engineering Materials Development Institute, Akure, Nigeria.
[1]Department of Materials Science and Engineering Obafemi Awolowo University, Ile Ife, Nigeria.
[2]Prototype Engineering Development Institute, Ilesa, Nigeria.

## ABSTRACT

The effect of strain rates on 0.19% C mild steel under tensile loading has been presented in this work. An electronic tensometer was used to conduct the test by varying the strain rates. Optical microscope and micro-hardness tester were used to characterize the microstructural orientations and hardness respectively around the necking region before and after test. From the results, the strain rate of 10 mm/min has proven to possess the highest hardness and lowest yield strength and hence, will give the optimum structural performance. The micrographs showed that 5 mm/min strain rate produced the least pearlite grains count, followed by that strained at 20 mm/min, then 30 mm/min and most pearlite grains count was found with that of strain rate 10 mm/min. Consequently, the area covered by ferrite grains was highest in 5 mm/min strain rate and least with that 10 mm/min strain rate.

**Keywords:** *strain rate, electronic tensometer, micrograph*

## 1. INTRODUCTION

The effect of the strain rate on the mechanical properties of materials is well known. Mechanical properties of metallic materials are affected by the strain rate and its effect on the compressive strength has been studied (Nemat-Nasser, 1994) showing an increase in strength with strain rate. The spalling test of long bars is a novel technique that provides the tensile strength of brittle materials at high strain rates under uniaxial stress conditions. This technique is based on the wave propagation in long bars and has been used by some authors (Johnstone et al., 1995; Gálvez Díaz-Rubio et al., 1997) who have studied and adopted an accepted method for maximizing the tensile property of materials by varying the strain rates.

In an attempt to improve on the mechanical properties of structural materials, tensile test has been one among the major tests required in assessing the tensile properties. Recently, this same method was being adopted on a special configuration for the evaluation of fracture toughness of any selected ferrous materials (Alaneme, 2011). Several tensile testing machineries have been produced for such test from manual to Computer Numeric Control (CNC) interface type. The results expected and gotten is agreed upon to have been influenced, among other factors, by the chosen or selected strain rate. Wiesner (1999) studied the loading rate effects on tensile properties and fracture toughness of steel and arrived at a conclusion that dynamic loading rates affect both the material resistance and the structural response of engineering components and it is the combination of these two influences that determines the structural behavior.

Generally, the effect of increasing loading rate is to increase strength and the strain rate sensitivity increases with temperature in steel and fiber (George and Antoine, 1985), but there are exceptions when dynamic strain ageing effects intervene (Wiesner, 1999). The behaviour of metals at strain rates from quasi-static to ultrahigh rate of deformed material was reviewed by Edward (2006).

## 2. MATERIALS AND METHOD

The material utilized for this research is a mild steel of 0.19% carbon composition. The as-received samples were machined to tensile test configuration of an average gauge length of 27mm and 3.6mm diameter with the aid of a medium size lathe machine. A ‘PC 2000’ electronic tensiometer was utilized to characterize the tensile properties at the different preselected strain rates ranging between 5 – 30mm/min. The samples were pulled to fracture and the results analyzed. Optical microscopy and microhardness tester were also used to evaluate the necking behavior at each strain rate. Prior to this characterization, the specimens were subjected to metallography processes that requires grinding with successive grits of grinding papers and then polished on a superfine polishing cloth on a Buehler grinding/polishing machine, and etched with 2% Nital following ASTM E2014 standard before capturing the micrographs with a daheng software driven microscope.

## 3. RESULTS AND DISCUSSION

Figure 1 shows the variation of microhardness value of the necking region of the specimen at different strain rates. It can be observed that the hardness value increased as the strain rate increased from 5 mm/min to optimal level of 20 mm/min and decreased at 30 mm/min. The resultant effect of the straining on the samples as compared to the control sample was the resultant increase in hardness value and can be improved by normalizing (Sanjib, 2009). This can be attributed to the type of crystal structure, structure reorientation and effect of strain (work) hardening mechanisms in different samples impacted by different strain rates. A reduction in dislocation tangle could be responsible for the result obtained at 30 mm/min.

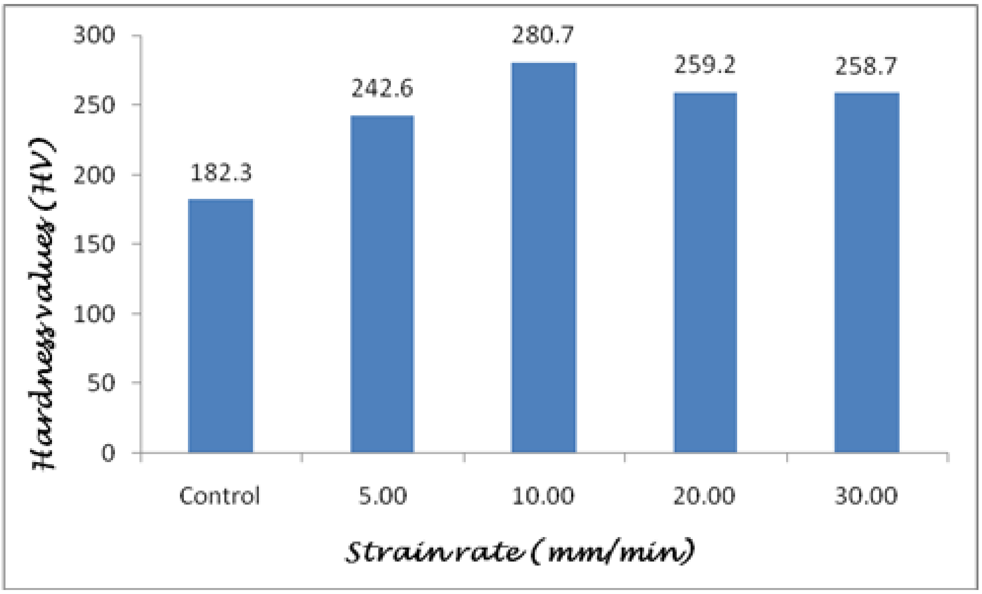


**Figure 1: Variation of Hardness with strain rates**

Figure 2(a) presents the graph of yield strength against strain rates. From the result, it can be observed that the specimens at 10, 20, and 30 mm/min strain rates had yield strength of 497 MPa, 544 MPa, and 550 MPa respectively with a steady increase. However, the specimen subjected to 5 mm/min strain rate had yield strength of 554 MPa having the highest value. This unexpected value may be attributed to alteration in the mechanical history that ensued in the course of machining this particular sample subjected to 5 mm/min. More importantly, early dislocation probably occurred in the specimen at 5 mm/min creating a displacement along the slip direction of the testing. Hence, the yield response produced the highest value.

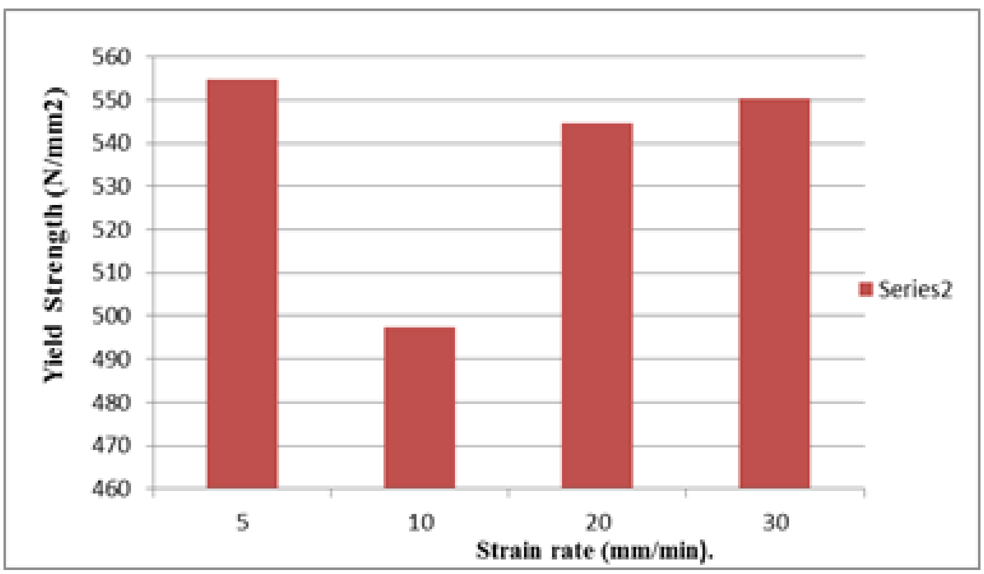


**Figure 2(a): Graph of yield strength against strain rates**

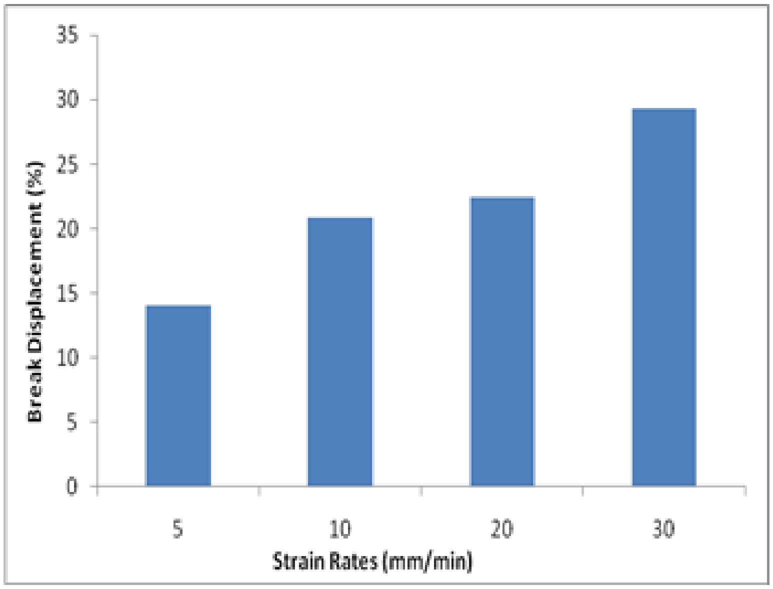


**Figure 2(b): Graph of Break Displacement versus strain rates**

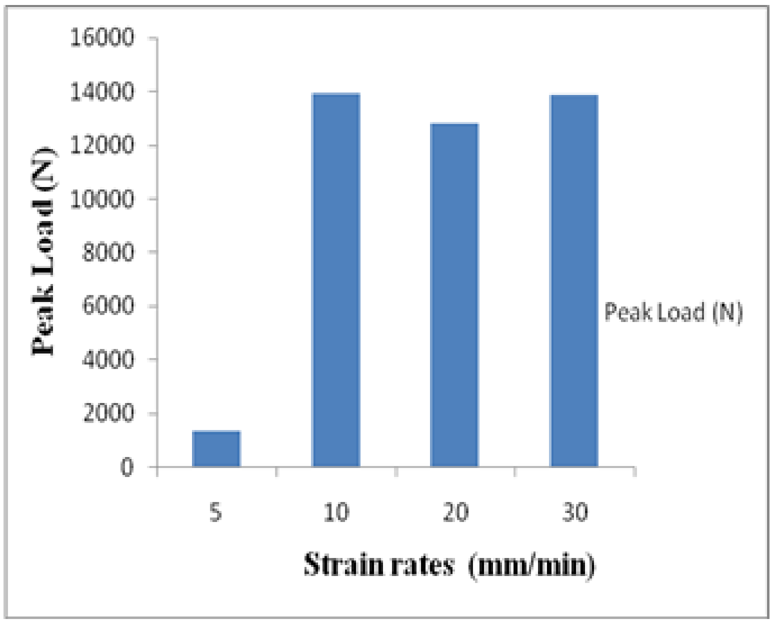


**Figure 3: Graph of Peak load versus strain rates**

The effect of strain rates on the peak load (maximum load) of different specimens is shown in Figure 3. The maximum load (UTS) of samples subjected to 5, 10, 20 and 30 mm/min strain rate was observed to be in order of 1,363.7 N; 13,916.1 N; 12, 827.6 N and 13, 896.5 N respectively.

Since all the specimens are of the same composition, the optimum strain rate for optimum UTS is 10 mm/min. This was followed by 30 mm/min.

Figure 4 shows the variation of engineering stress to strain. From the result, it was observed that most of the plots exhibited continuous yield typical of traditional mild steel compositions. The reason has been traced to the bcc (body centered cubic) structure of the material (Armstron and Walley, 2008). The discontinuous yielding due to presence of definite yield point phenomenon observed in specimen subjected to 10mm/min strain rate, however, could be due to phase straining (plastic deformation) induced in the microstructure [Park et al., (2005) and Alaneme (2010)] during machining. These unique behaviors in tensile properties define homogeneous strain hardening characteristic of mild steel, showing good agreement with the results obtained in microstructures before and after necking.

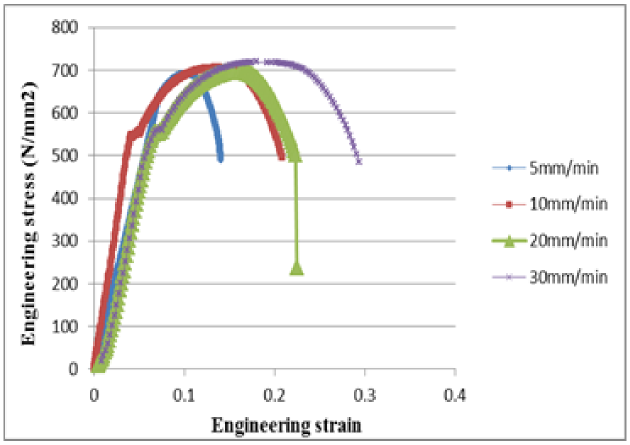


**Fig. 4: Graph of Engineering stress to strain for different strain rates**

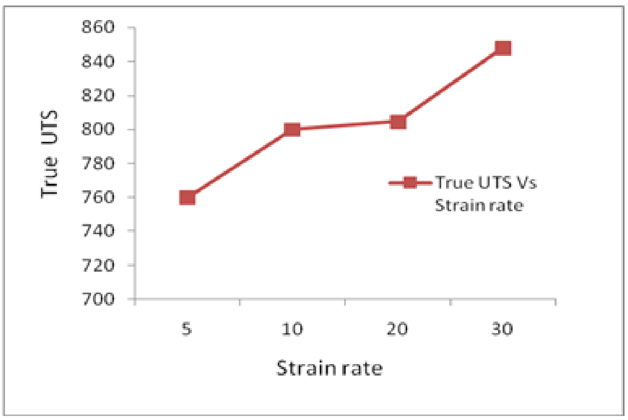


**Fig. 5: Graph of True UTS for different strain rates**

Figure 5 is a graph of true UTS for different strain rates. It shows that as the strain rate increases, the true Ultimate Tensile Strength increases. At the strain rate of 30mm/ min, the highest true UTS of 848.1 $Nmm^{-2}$ was observed.

To analyze the possible changes in the tension mode, a micrograph analysis of the necking region was done using daheng software driven optical microscope. The microstructures were observed not to be significantly affected or altered in any form from its conventional known ferrite (grey phase) and cementite (dark phase) at almost equal volume percentage in spite of the varying strain rates. Plate 1 (control) showed more visible grain boundaries than in plate 2 (strain rate of 5 mm/min). There is a certain degree of grain refinement conferred on plate 2 as a result of straining. Plate 3 has the highest degree of grain refinement conferred, hence, confirming the highest hardness as shown in Figure 1 and lowest yield strength as presented in figure 2 (a) above.

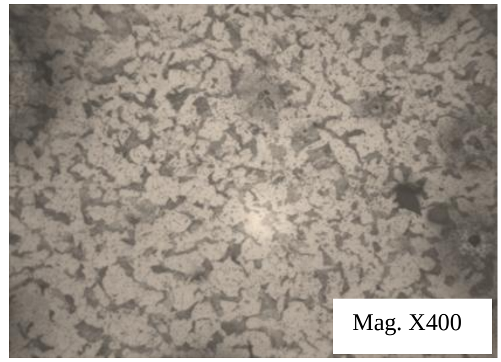


**Plate 1: Micrograph of control sample before subjecting it tension on e-tensometer**

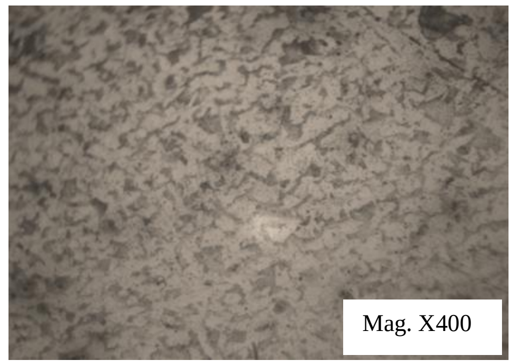


**Plate 2: Micrograph of necking region strained at 5mm/min on e-tensometer**

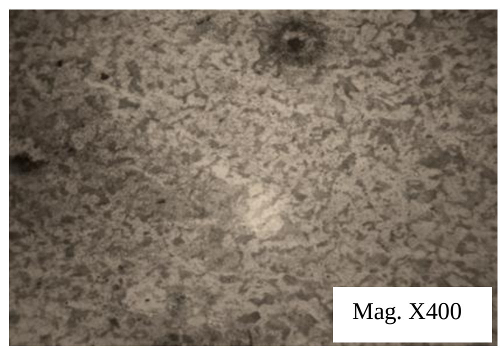


**Plate 3: Micrograph of necking region strained at 10mm/min on e-tensometer**

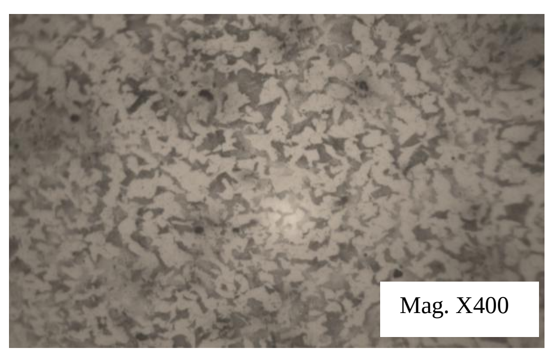


**Plate 5: Micrograph of necking region strained at 30mm/min on e-tensometer**

## 4. CONCLUSION

The tensile and microstructural properties of mild steel of carbon composition 0.19% have been studied by varying the strain rates, with initial emphasis on its necking behavior. From the results, it was observed that most of the specimens yielded continuously as the strength consistently increased with respect to the selected strain rate. The strain rate of 10 mm/min has proven to possess the highest hardness and peak load but lowest yield strength. The elongation was observed to increase as the strain rates increase. The micrographs showed that 5 mm/min strain rate produced the least pearlite grains count, followed by that strained at 20 mm/min, then 30 mm/min and most pearlite grains count was found with that of strain rate 10 mm/min. Consequently, the area covered by ferrite grains was highest in 5 mm/min strain rate and least with that 10 mm/min strain rate. Mild steel with 0.19%C will display optimum structural performance under loading rate of 10mm/min.

## REFERENCES

[1] Alaneme K.K (2010): Influence of Tempered Microstructures on the Transformation Behaviour of Cold Deformed and Intercritically Annealed Medium Carbon Low Alloy Steel. Material Research. Pp. 1516 – 1518.

[2] Alaneme K.K (2011): Fracture Toughness ($K_{1C}$) Evaluation for Dual Phase Medium Carbon Low Alloy Steels Using Circumferential Notched Tensile (CNT) Specimens. Materials research; 14(2): 155-160.

[3] Edwards M. (2006): Ingentaconnect properties of metals at high rates of strain. Materials Science and Technology. Maney publishing. Vol. 22. No. 4 Pp. 453-462.

[4] Lankford J. (1981):"Temperature-strain rate dependance of compressive strength and damage mechanisms in aluminium oxide". J. of Mat. Sci. 16 pp. 1567-1578.

[5] Wiesner C.S. and MacGilliavray H. (1999): Loading Rate Effects on Tensile Properties and Fracture Toughness of Steel. Presented at 1999 TAGSI Seminar. Held at TWI, Cambridge, UK, 29 April, 1999.

[6] George G. and Antoine N. (1985): Strain Rate Effects on Tensile Properties of Fiber Reinforced Concrete. MRS Proceedings. Vol. 64. 22 pages.

[7] Gálvez Díaz-Rubio F., Rodríguez J., Sánchez-Gálvez, (1997) "Tensile Strength Measurements of Ceramic Materials at High Rates of Strain". Journal de Physique IV, Colloque C3 Supplément au Journal de Physique III, nº7, pp.151-156 d'Août.

[8] Nemat-Nasser S., Deng H. (1994) : "Strain rate effect on brittle failure in compression". Acta metall. mater. Vol42, No 3, pp 1013-1024.

[9] Neville A.M. (1973) "Properties of concrete". Pitman publishing...

[10] Ovri J.E.O., Davies T. J. 1987: "Diametral compression of silicon nitride". Materials Science and Engineering. 96, pp 109-116.

[11] Park .K, Lee .C. S, and Shin .D. H (2005): Strain Hardenability of Ultra fine Grained low Carbon Steels Processed by ECAP, Rev. Adv. Mater. Science (10) pp 133 – 137.

[12] Sanjib, K.J. (2009) Heat Treatment Of Low Carbon Steel Bachelor of Technology (Mechanical Engineering) Thesis, Department of Mechanical Engineering National Institute of Technology Rourkela-769008

# APPENDIX

**Table: 1 Summary of tensile properties at various strain rates using electronics tensiometer**

| Strain rate | Engineering stress vs Engineering strain | Load vs displacement | True stress vs true strain |
|---|---|---|---|
| **5mm/min**. | | | |
| Yield strength (N/mm$^2$) | 554.61 | 560.280 | 594 |
| Work done (Nmm) | 11039.4 | 11039.4 | 11039.4 |
| Proof stress (N/mm$^2$) | 641.5 | 641.5 | 641.5 |
| Peak load (N) | 1363.7 | 1363.7 | 1363.7 |
| Break load (N) | 9650.1 | 9650.1 | 9650.1 |
| Slope (N/mm) | 1.8 | 1.8 | 1.8 |
| Fracture strength (N/mm$^2$) | 489.306 | 489.306 | 489.306 |
| Strain until fracture | 0.14 | 0.14 | 0.14 |
| Peak displacement (mm) | 2.61 | 2.61 | 2.61 |
| Break displacement (mm) | 3.70 | 3.70 | 3.70 |
| Peak displacement (%) | 9.93 | 9.93 | 9.93 |
| Break displacement (%) | 14.05 | 14.05 | 14.05 |
| **10mm/min.** | | | |
| Yield strength (N/mm$^2$) | 497.262 | 530.579 | 590.5 |
| Work done (Nmm) | 5335.5 | 5335.5 | 5335.5 |
| Proof stress (N/mm$^2$) | 544.0 | 544.0 | 544.0 |
| Peak load (N) | 13916.1 | 13916.1 | 13916.1 |
| Break load (N) | 9807.0 | 9807.0 | 9807.0 |
| Slope (N/mm) | 3.9 | 3.9 | 3.9 |
| Fracture strength (N/mm$^2$) | 497.261 | 497.261 | 497.261 |
| Strain until fracture | 0.22 | 0.22 | 0.22 |
| Peak displacement (mm) | 3.34 | 3.34 | 3.34 |
| Break displacement (mm) | 5.21 | 5.21 | 5.21 |
| Peak displacement (%) | 13.36 | 13.36 | 13.36 |
| Break displacement (%) | 20.82 | 20.82 | 20.82 |
| **20mm/min.** | | | |
| Yield strength (N/mm$^2$) | 544.54 | 544.537 | 579.75 |
| Work done (Nmm) | 10909 | 10909 | 10909 |
| Proof stress (N/mm$^2$) | ---------- | ---------- | --------- |
| Peak load (N) | 12827.6 | 12827.6 | 12827.6 |
| Break load (N) | 4393.5 | 4393.5 | 4393.5 |
| Slope (N/mm) | 2.7 | 2.7 | 2.7 |
| Fracture strength (N/mm$^2$) | 238.699 | 238.699 | 238.699 |
| Strain until fracture | 0.24 | 0.24 | 0.24 |
| Peak displacement (mm) | 4.11 | 4.11 | 4.11 |
| Break displacement (mm) | 5.98 | 5.98 | 5.98 |
| Peak displacement (%) | 15.45 | 15.45 | 15.45 |
| Break displacement (%) | 22.48 | 22.48 | 22.48 |
| **30mm/min.** | | | |
| Yield strength (N/mm$^2$) | 550.470 | 550.470 | 494.64 |
| Workdone (Nmm) | 57138.2 | 57138.2 | 57138.2 |

| | | | |
|---|---|---|---|
| Proof stress ($N/mm^2$) | 650.4 | 650.4 | 650.4 |
| Peak load (N) | 13896.5 | 13896.5 | 13896.5 |
| Break load (N) | 9375.5 | 9375.5 | 9375.5 |
| Slope (N/mm) | 2.9 | 2.9 | 2.9 |
| Fracture Strength ($N/mm^2$) | 485.023 | 485.023 | 485.023 |
| Strain until fracture | 0.31 | 0.31 | 0.31 |
| Peak displacement (mm) | 4.44 | 4.44 | 4.44 |
| Break displacement (mm) | 7.25 | 7.25 | 7.25 |
| Peak displacement (%) | 17.98 | 17.98 | 17.98 |
| Break displacement (%) | 29.35 | 29.35 | 29.35 |